Experimental investigation of a new CO2 refrigeration system arrangement for supermarket applications

Ana Paez, Bénédicte Ballot-Miguet, Benoit Michel, Pascal Tobaly, Rémi Revellin

▶ **To cite this version:**

Ana Paez, Bénédicte Ballot-Miguet, Benoit Michel, Pascal Tobaly, Rémi Revellin. Experimental investigation of a new CO2 refrigeration system arrangement for supermarket applications. International Journal of Refrigeration, 2024, 162, pp.245 - 256. ⟨10.1016/j.ijrefrig.2024.03.010⟩. ⟨hal-04593979⟩

HAL Id: hal-04593979

https://hal.science/hal-04593979v1

Submitted on 5 Jul 2024

HAL is a multi-disciplinary open access archive for the deposit and dissemination of scientific research documents, whether they are published or not. The documents may come from teaching and research institutions in France or abroad, or from public or private research centers.

L'archive ouverte pluridisciplinaire **HAL**, est destinée au dépôt et à la diffusion de documents scientifiques de niveau recherche, publiés ou non, émanant des établissements d'enseignement et de recherche français ou étrangers, des laboratoires publics ou privés.

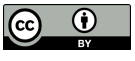

Distributed under a Creative Commons CC BY 4.0 - Attribution - International License

International Journal of Refrigeration 162 (2024) 245–256

Contents lists available at ScienceDirect

International Journal of Refrigeration

journal homepage: www.elsevier.com/locate/ijrefrig

Experimental investigation of a new CO_2 refrigeration system arrangement for supermarket applications

Étude expérimentale d'un nouveau système frigorifique au CO_2 pour les supermarchés

Ana Paez [a,b,c,d,*], Bénédicte Ballot-Miguet [d], Benoit Michel [a], Pascal Tobaly [b,c], Rémi Revellin [a]

[a] Univ Lyon, INSA Lyon, CNRS, CETHIL, UMR5008, 69621, Villeurbanne, France
[b] LaFSET, Laboratoire du Froid, des Systèmes Energétiques et Thermiques, Paris, 75003, France
[c] Université Sorbonne Paris Nord, Villetaneuse, 93430, France
[d] EDF R&D, Écuelles, 77250, France

ARTICLE INFO

Keywords:
CO_2, Refrigeration system
Internal heat exchanger
Reduced superheat
Energy efficiency and experimentation

Mots clés:
CO2 Système frigorifique
Échangeur de chaleur interne
Surchauffe réduite
Efficacité énergétique
Expérimentation

ABSTRACT

A new position of an internal heat exchanger within the thermodynamic cycle is proposed to improve the performance of CO_2 refrigeration systems in warm climates, specifically in supermarket applications. The proposed configuration uses the saturated vapor from the liquid receiver to recover the heat that is rejected by a subcooler positioned after the gas cooler. This system results in a reduced evaporator superheat. This configuration is compared with a reference system.

The experimental study is conducted on a CO_2 laboratory cooling system reproducing a commercial plant. The cooling capacity of the system is 30 kW. The water inlet temperature in the gas cooler (hot source) varies from 15 °C to 35 °C, while the mono-ethylene glycol outlet temperature of the evaporator (cold source) is fixed at -8 °C. The setup is validated through an energy balance.

Using a subcooler in this new position improves the coefficient of performance by 10.2 % under transcritical conditions and 6.3 % under subcritical conditions when compared with the reference system.

1. Introduction

Nowadays, an accelerated climate change is observed, which is caused by several human activities such as agriculture, transportation, electricity production and land use. These activities increase greenhouse gas emissions (IPCC, 2023). One part of additional greenhouse gasses emissions is due to the use of certain refrigerants used in heating and cooling sectors.

In order to mitigate the environmental impact, the F-gas regulation was introduced in the European Union in 2006 following the Kyoto Protocol, with the aim of restricting the use of hydrofluorocarbon (HFC) refrigerants. The F-gas 2014 regulation specifically prohibits, since January 1, 2022, the use of HFC refrigerants with Global Warming Potentials (GWPs) exceeding 150 in new commercial refrigeration systems. This regulation and the changes made in the latest version (F-gas 2023) have fostered the exploration and adoption of natural refrigerants such as CO_2, water, air, ammonia, ethyl ethers, propane, and others as alternatives.

The European refrigeration community is looking for climate-friendly and lower energy-consuming alternative refrigerants. The CO_2 becomes a good candidate because it has zero ozone depletion potential, has a very low global warming potential, is non-flammable and nontoxic. However, its performances in warm climate conditions should be improved to reduce the energy consumption and to be more energy efficiently attractive.

Different alternatives have been proposed in the literature to increase the CO_2 cooling systems performance. Some of them consist in adding some equipment in the cycle, for example, an internal heat exchanger in different positions (Karampour and Sawalha, 2014; S. S. Liu et al., 2021; Llopis et al., 2018; Rigola et al., 2010; Sánchez et al., 2014; Yu et al., 2019a), a mechanical subcooling (X. S. Liu et al., 2021; Llopis et al., 2018, R. 2016; Nebot-andrés et al., 2022a), a mechanical subcooling with an ejector (Dai et al., 2023), a parallel compressor (Chesi et al., 2014; Sacasas et al., 2022), an expander (Ma et al., 2013; Yang et al., 2005; Yu et al., 2019b), an ejector (Deng et al., 2007;

* Corresponding author.
E-mail address: ana.paez@edf.fr (A. Paez).

https://doi.org/10.1016/j.ijrefrig.2024.03.010
Received 1 December 2023; Received in revised form 28 February 2024; Accepted 15 March 2024
Available online 16 March 2024
0140-7007/© 2024 The Authors. Published by Elsevier B.V. This is an open access article under the CC BY license (http://creativecommons.org/licenses/by/4.0/).

Nomenclature

Abbreviations

COP	Coefficient of performance
CP	Compressor
EV	Expansion valve
FGV	Flash gas valve
GC	Gas cooler
GWP	Global warming potential
HP	High pressure (bar)
HPV	High pressure valve
HX	Evaporator
LP	Low pressure (bar)
LR	Liquid receiver
MEG	Mono-ethylene glycol
MP	Medium pressure (bar)
N.A	Not available
OR	Oil receiver
OS	Oil separator
PI	Proportional-integral
REF	Reference system
RTD	Resistance temperature detectors
SC	Subcooler

Subscripts

out	Outlet
In	Inlet

Symbols

cp	Specific heat capacity (J/g K)
h	Specific enthalpy (kJ/kg)
$\dot{m}$	Mass flow rate (kg/s)
P	Pressure (bar)
$P_{evap\_electric}$	Electrical resistance power (kW)
P_{elec}	Compressor electric power (kW)
$\dot{Q}_{evap}$	Cooling capacity (kW)
$\dot{Q}_{GC}$	Heat capacity (kW)
T	Temperature (°C)
U_c^2	Combined uncertainty
$u(x_i)$	Uncertainty

Fangtian and Yitai, 2011; Ksayer and Clodic, 2006; Li and Groll, 2005; Liu et al., 2012; Nakagawa et al., 2010), an ejector with an internal heat exchanger (Elbel and Hrnjak, 2004; M. Masafumi Nakagawa et al., 2011; Masafumi M. Nakagawa et al., 2011; Xu et al., 2011; Zhang et al., 2013), or a multi-ejector (Elbarghthi et al., 2021; Hafner et al., 2014; Haida et al., 2020; X. S. Liu et al., 2021; Pardiñas et al., 2023, 2022; Singh et al., 2021, 2020). Another proposed approach involves operating under reduced superheat conditions. This reduces the temperature difference between the two fluids in the evaporator and increases the heat transfer coefficients. Consequently, this leads to an improved evaporator efficiency (Minetto et al., 2014; Singh et al., 2020).

However, working with reduced superheat conditions implies adding equipment to prevent any evaporator outlet liquid from reaching the compressors. To manage this problem, diverse solutions have been proposed like adding a single-phase ejector (Gullo et al., 2017; Haida et al., 2020; Minetto et al., 2014; Singh et al., 2020), a pump (Gullo et al., 2016) or a two-level evaporation (Cavalleri et al., 2019; Paolo 2016). However, these solutions require an extra control system.

Using mechanical subcooling alone or in combination with an ejector makes the system more complex and requires an additional system using refrigerant fluid, or the addition of a parallel compressor (Nebot-Andrés et al., 2022b), which increases installation costs.

Ejector solutions seem like a very good idea to improve COP, especially the use of a two-phase ejector or multi-ejector technology. But these are complex technologies that not all maintenance personnel are familiar with. These technologies also require a more complex control of the installation to keep it stable, without many oscillations that can degrade the performance of the machine.

Therefore, adding an internal heat exchanger is an interesting solution of which effective operation does not demand specialized knowledge or additional control. Different positions of the internal heat exchanger in the thermodynamic cycle have been studied as previously mentioned. Most of them are experimental analyses with low cooling capacity (< 10 kW) (Aprea and Maiorino, 2008; Cabello et al., 2008; Kim et al., 2017, 2005; Rigola et al., 2010; Sánchez et al., 2014; Tao et al., 2010), those of high cooling capacity are two-stage cycles (Karampour and Sawalha, 2014; S. S. Liu et al., 2021; Sawalha et al., 2015). To the best of our knowledge, there is no experimental study, whether for low or high cooling capacity, that uses an internal heat exchanger located at the outlet of the gas cooler and using the saturated vapor leaving the intermediate liquid receiver, along with a reduced superheat.

The main objective of this article is to contribute to the literature with a new position of the internal heat exchanger using a reduced superheat condition in a transcritical CO_2 single-stage system. The performance of this system is evaluated against a reference system at different ambient temperatures in an experimental setup. The ambient temperatures are simulated with a water loop.

The article is divided into two parts. The first part describes the 30 kW cooling capacity test facility, its components and the uncertainties of the measurements. The second part corresponds to the experimental setup validation and the results for both CO_2 refrigeration systems: the reference system and the proposed system. Finally, the conclusions are presented.

2. Experimental setup

Fig. 1 and Fig. 2 show the schema and the photo of the transcritical CO_2 test facility composed by three main closed circuits: water circuit (green), mono-ethylene glycol (MEG) circuit (pink) and refrigerant system (CO_2). The first loop (water circuit) is used to absorb the heat rejected by the gas cooler and simulate different ambient temperatures. The second loop (MEG circuit) is used to simulate the cooling capacity demand, it uses an electrical resistance for this purpose. Finally, the refrigeration CO_2 system is composed by three reciprocating compressors (CP), a gas cooler (GC), an oil separator (OS), an oil receiver (OR), an internal heat exchanger used as subcooler (SC), a liquid receiver (LR), an evaporator (HX), a high pressure valve (HPV), a flash gas valve (FGV) and an expansion valve (EV). The oil separator is used to separate the refrigerant from the oil used in the compressors' lubrication. By the use of by-passes, two arrangements are possible in this CO_2 test facility as will be explained in Section 2.3.1 (reference system) and Section 2.3.2 (subcooling system). The valves 1 and 2 of Fig. 1 are used to switch between the operation modes of the installation. When valve number 1 is open and valve number 2 is closed, the subcooler is used. When valve number 2 is open, and valve number 1 is closed the reference system is used. The three different pressure levels are represented in red, orange and blue for the high, medium and low pressure respectively.

The gas cooler and evaporator are brazed plate heat exchangers. Their geometries are presented in Table 1. The subcooler is a tube and shell heat exchanger, its heat transfer area is 0.2309 m^2 with 10 tubes of 8 mm and 10 mm for inner and outer diameters respectively.

The three compressors installed in the test facility are semi-hermetic four cylinders compressors from Dorin, two of them are equipped with

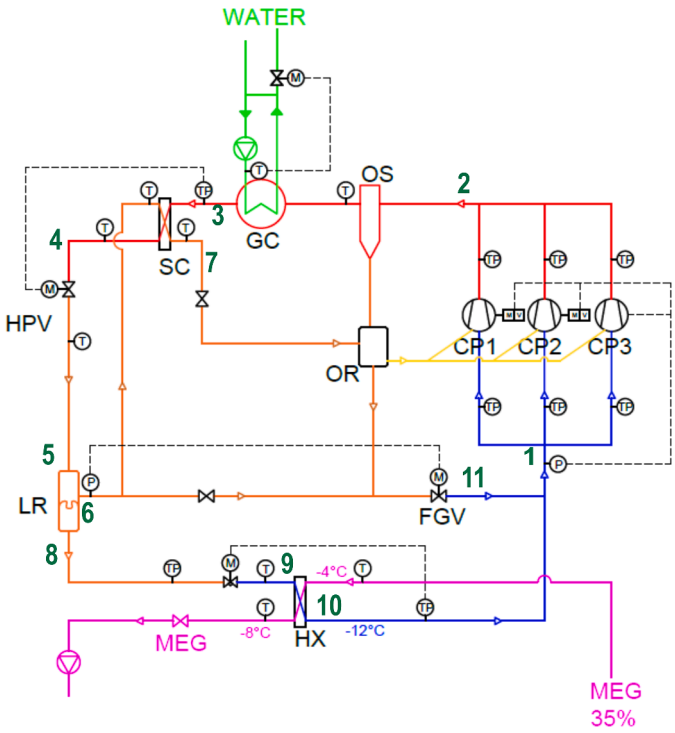

Fig. 1. Transcritical CO_2 test facility. Water loop (green), MEG loop (pink) and CO_2 circuit with the three pressure levels highlighted, red, orange and blue for the high, the medium and the low pressure respectively. The yellow lines represent the oil supply to the compressors. T and P are temperature and pressure sensors. M represents a motorized valve and the dotted lines represent the control system. The green numbers will be useful in Fig. 4.

an inverter drive.

The expansion valves are CCMT4 valves from Danfoss.

2.1. Regulation system

There are five proportional-integral (PI) regulation systems installed in the test facility to control the evaporation pressure, the superheat, the liquid receiver pressure, the optimal high pressure and the desired gas cooler inlet water temperature.

The evaporation pressure or low pressure is controlled by the three main compressors installed in the machine. These compressors operate in a rotating manner to ensure equal usage over time.

The control of the compressors' power to reach a specific low pressure is influenced by three factors: the number of compressors activated, the compressors' motor speed and a neutral zone. Compressor speed is controlled by two inverters installed on two of three compressors. The neutral zone, often referred to as the "dead band," constitutes a range around the setpoint where there is no variation in power demand, thereby upholding system stability. For optimal stability, the dead band is set at 0.5 bar.

The superheat and the liquid receiver pressure are controlled by the two Danfoss CCMT4 motorized valves: EV for the superheat value and FGV for the liquid receiver pressure.

The high-pressure control represents a big challenge in all CO_2 transcritical machines because of its thermodynamic properties, mainly its critical temperature and the high temperature variation due related to small pressure changes.

CO_2 systems have two fundamental operational states: the subcritical and the transcritical regimes.

To ensure a smooth transition from the subcritical to the transcritical regime, a transition zone must be defined. This transition zone plays an important role in the high-pressure control strategy. In this paper, the transition zone is delimited by pressures ranging from 61 bar to 83 bar, corresponding to CO_2 outlet temperatures from the gas cooler within the interval of 20 °C to 31 °C.

This approach ensures the correct system operation at all water inlet temperatures. Fig. 3 shows the three main operating regimes for CO_2: the subcritical regime (high-pressure below 61 bar), the transition zone (high-pressure between 61 bar and 83 bar), and the transcritical regime (high-pressure above 83 bar).

The high pressure of the system is variable to achieve a good performance. It uses polynomial equations based on the CO_2 outlet temperature from the gas cooler ($T_{out\_CO_2\_GC}$). The CO_2 outlet temperature is the result of the heat transfer in the gas cooler, hence temperature oscillations can be observed with small pressure changes. To maintain a stable operating condition, faster control is required. Consequently, an advanced control is used instead of the conventional industry PI control for the high pressure control. This advanced control was previously developed by EDF (Électricité de France) (Ballot-Miguet et al., 2016; Changenet et al., 2008; Fallahsohi et al., 2010a, 2010b).

The specific polynomial equations for each operational mode are

Table 1
Brazed plate for gas cooler and evaporator heat exchangers.

Parameter	Gas cooler	Evaporator
Volume by channel (L)	0.095	0.18
N° plates	90	60
Width (m)	0.05	0.092
Length (m)	0.466	0.519
Heat transfer area (m^2)	4.49	6.5

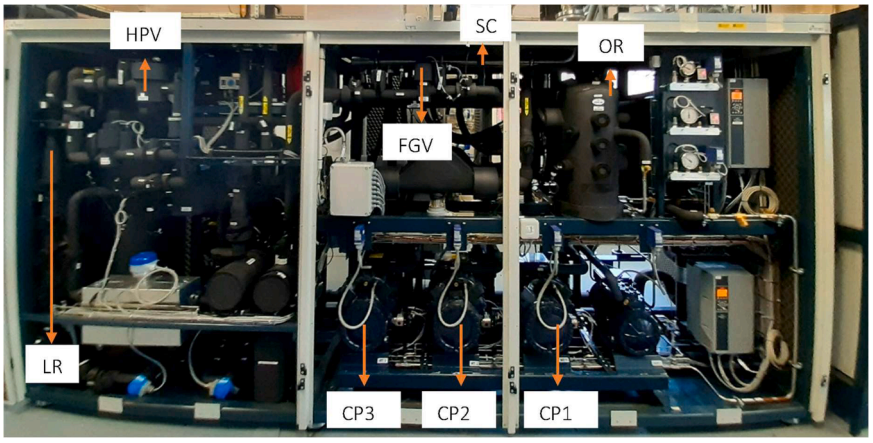

Fig. 2. Test facility.

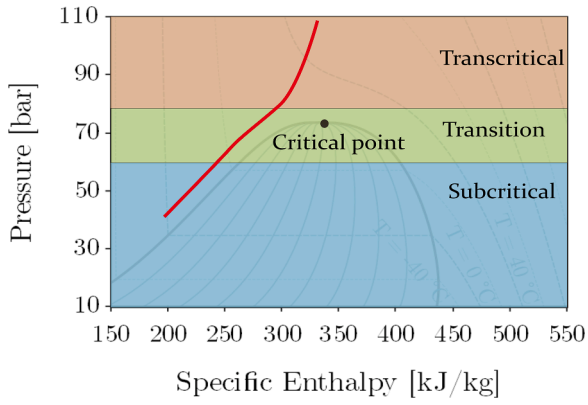

Fig. 3. Three operating regimes for CO_2.

presented in Table 2. They are the result of a linear regression of the limits established for the transcritical zone and the maximum high pressure (104 bar).

2.2. Instrumentation

The three main loops are fully instrumented with flowmeters, temperature and pressure sensors (Table 3). The main sensor locations are shown in Fig. 1.

The expanded uncertainty of each sensor presented in Table 3 considers all the measuring chain, which means the sensor and the automate errors. The expanded uncertainty takes a factor of 2 that corresponds to a confidence interval of 95%.

When a calculation includes several variables, for example the calculation of the coefficient of performance, a combined standard uncertainty (U_c^2) should be calculated (Eq. (1)). The method is based on first-order Taylor series, and it is referred to as the law of propagation of uncertainty (Taylor, Barry N and Kuyatt, 1994).

$$U_c^2(y) = \sum_{i=1}^{n} \left(\frac{\partial f}{\partial x_i}\right)^2 u^2(x_i) \tag{1}$$

where $u(x_i)$ is the uncertainty of each variable.

To compute uncertainties related to thermodynamic properties like enthalpy and heat capacity, the approach established by Moffat et al. (Moffat, 1982) has been adopted. This methodology primarily involves numerically determining the uncertainty associated with a function by considering the individual contributions to uncertainty from each variable involved in the measured function (see Eqs. (2), (3) and (4)).

$$u(h) = \sqrt{\left(\frac{\partial h}{\partial T} \times \Delta T\right)^2 + \left(\frac{\partial h}{\partial P} \times \Delta P\right)^2} \tag{2}$$

$$\frac{\partial h}{\partial T} = \frac{h_{(T + u(T))} - h_{(T - u(T))}}{2u(T)} \tag{3}$$

$$\frac{\partial h}{\partial P} = \frac{h_{(P + u(P))} - h_{(P - u(P))}}{2u(P)} \tag{4}$$

$u(h)$ is the uncertainty of enthalpy, T is the temperature, P is the pressure, $u(T)$ and $u(P)$ are the uncertainties of temperature and pressure respectively.

Table 2
High pressure control.

Conditions	Equations
Subcritical ($T_{out\_CO_2\_GC} < 20$ °C)	$HP\ (bar) = T_{out\_CO_2\_GC} \times 1.21 + 34.89$
Transition ($T_{out\_CO_2\_GC} > 20$ °C and < 31 °C)	$HP\ (bar) = T_{out\_CO_2\_GC} \times 2.1 + 17.2$
Transcritical ($T_{out\_CO_2\_GC} > 31$ °C)	$HP\ (bar) = T_{out\_CO_2\_GC} \times 2.5 + 4.5$

Table 3
Sensor information.

Sensor	Brand	Model	Class	Range	Uncertainty
Pressure (HP) (bar)	Carel	SPKT00D8C0	–	0; 150	± 0.85
Pressure (MP) (bar)	Danfoss	AKS 32	–	−1; 59	± 0.31
Pressure (LP) (bar)	Carel	SPKT00G1C0	–	0; 60	± 0.25
Temperature RTD (MEG) (°C)	TCSA	PT100	1/10	N.A	± 0.070
Temperature RTD (CO_2) (°C)	Danfoss	PT1000 AKS11	B	10; 140	± 0.71
Temperature RTD (CO_2) (°C)	TCSA	PT1000	B	−20; 10	± 0.37
Temperature RTD (water) (°C)	TCSA	PT100	1/10	N.A	± 0.073
Flowmeter (kg/s)	Krohne	OPTIMASS	–	Max 0.3	±0.0011
Wattmeter (kW)	Diris	N.A	N.A	N.A	± 0.10

N.A = Not available.

2.3. CO_2 refrigeration systems

2.3.1. Reference system

Fig. 4 shows the simplified diagram and the thermodynamic cycle of the reference system in an enthalpy-pressure diagram. The CO_2 vapor coming out from the compressors is cooled in the gas cooler (GC), and it is expanded through the high-pressure valve (HPV) from high-pressure to medium-pressure. The two-phase fluid resulting from the throttling process enters the intermediate liquid receiver (LR). The vapor is expanded by the flash gas valve (FGV) to reduce its pressure from medium to low (evaporation) pressure. The liquid is expanded through the expansion valve and passes through the evaporator (HX). The flash gas valve and evaporator outlet fluids are mixed before reaching the compressors inlet.

Reducing the evaporator superheat in this system is not feasible due to the associated risk of compressor damage from excess liquid.

This system is considered as already improved because of the following reasons:

- It is provided with an intermediate liquid receiver on a medium-pressure level which allows to reduce the evaporator inlet vapor quality. Furthermore, it allows separate controls of optimum high pressure (point 3, Fig. 4) and superheat control (point 10, Fig. 4).
- It works with optimal high pressure (Section 2.1). In transcritical conditions the high pressure set value changes as a function of the gas cooler outlet CO_2 temperature to obtain the maximum COP. In subcritical conditions, the system seeks to maintain 2 °C subcooling at the exit of the gas cooler.
- A moderate evaporator superheat is used, 8 °C, which is lower than usually used in the commercial applications.
- The system is equipped with two inverter drives that regulate the compressors' frequencies to maintain the desired evaporator secondary fluid outlet temperature.

2.3.2. Internal heat exchanger (subcooling) system

The second system involves the addition of an internal heat exchanger to the reference system (Fig. 5(a)). It is located at the outlet of the gas cooler (high pressure side) and at the vapor outlet of the liquid receiver (medium-pressure side). Unlike the conventional application of internal heat exchangers suggested in the literature (Aprea and Maiorino, 2008; S. S. Liu et al., 2021; Nebot-Andrés, 2022; Rigola et al., 2010; Sánchez et al., 2014), this system uses saturated vapor from the liquid receiver to recover the heat rejected by the subcooler, rather than the fluid leaving the evaporator.

This system is used with an evaporator superheat of 8 °C (like the

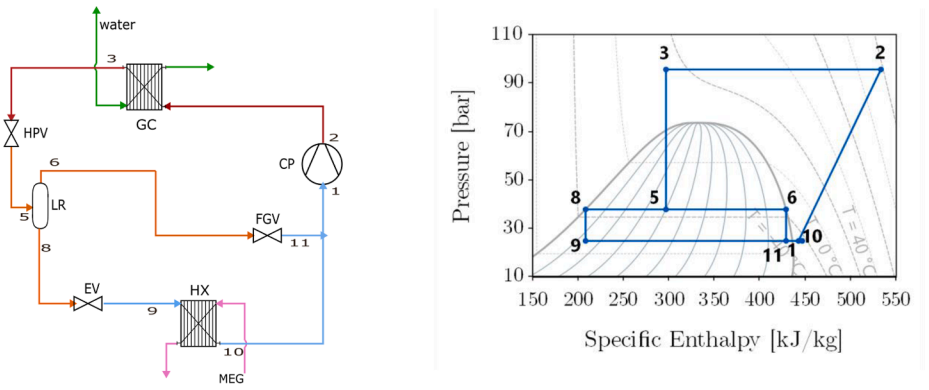

a) Simplified diagram b) Enthalpy-pressure diagram

Fig. 4. Reference system.

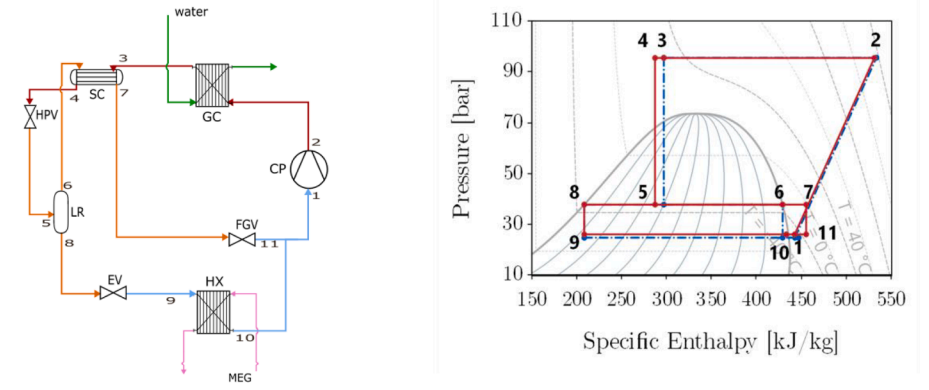

a) Simplified diagram of subcooling system b) Enthalpy-pressure diagram (red lines) and reference system (blue lines)

Fig. 5. Subcooling system.

reference system) and with a reduced evaporator superheat of 1.8 °C (flooded evaporator).

Flooded conditions can be used with this configuration without risking compressor damage, as the superheated vapor at the flash gas valve outlet (point 11) is utilized to evaporate the excess liquid from the evaporator.

The main advantage to use a subcooler in this position is to reduce the total mass flow rate for a given cooling capacity. Additionally, when flooded conditions are used, the evaporator pressure is increased which reduces compressor power consumption.

It is important to know that the heat transferred in the subcooler is influenced by subcooler dimensions. In the tested conditions with the given subcooler dimensions, no excess liquid was observed at the compressor inlet when a reduced superheat was used. However, this configuration should be carefully evaluated in other machines to appropriately size the subcooler depending on the application.

2.4. Experimental conditions

The experimental results are obtained under the following conditions:

The water inlet temperatures in the gas cooler vary between 15 °C and 35 °C using the control system showed in Fig. 1. The water mass flow rate is kept constant at 2.1 kg/s.

The mono-ethylene glycol (MEG) temperature at the evaporator outlet and its mass flow rate are fixed at -8 °C and 2.3 kg/s respectively to keep constant the 30 kW cooling capacity. The cooling demand is provided by an electrical resistance that heats the MEG fluid.

The high pressure set value is established according to polynomial functions of the CO_2 outlet temperature of the gas cooler described in Section 2.1.

The receiver pressure is fixed at 38 bar as it will be explained in Section 2.5.

In the subcooling system, the superheat is tested at 1.8 °C and 8 °C, whereas in the reference system, it is fixed at 8 °C. The presence of the subcooler allows to reduce the superheat in the system without the risk of liquid droplets entering the compressors thanks to advantages mentioned in Section 2.3.2.

The data are collected every 10 s during 50 min after the stationary conditions are reached. In order to reduce the error and ensure the data reliability, the values used are the average results of at least five repetitions of each experiment for both configurations.

The COP calculated in this article is the ratio between the power provided by the electrical resistance ($P_{evap\_electric}$) and the compressors electrical consumption (P_{elec}) as shown in Eq. (5).

$$COP = \frac{P_{evap\_electric}}{P_{elec}} \tag{5}$$

2.5. Variation of medium and high pressures

The impact of gas cooler pressure (high-pressure) and liquid receiver pressure (medium-pressure) on the system performance was studied. These two factors were tested independently. For a water inlet temperature to the gas cooler of 25 °C, the gas cooler pressure ranged from 70 to 77 bar while maintaining a constant medium pressure of 38 bar. Subsequently, the medium pressure varied from 32 to 44 bar with a

constant high pressure of 74 bar. Similarly, for a water inlet temperature to the gas cooler of 30 °C, the pressure variation in the gas cooler oscillated between 77 and 87 bar with a constant medium pressure of 38 bar, and the medium pressure between 32 and 44 bar with a constant high pressure of 84 bar.

Fig. 6 depicts the variation of the COP versus the two pressures. Medium-pressure had no significant impact on the system performance, while high-pressure had a visible impact. In this last case, an optimal value is observed. It was therefore decided to work with a constant medium-pressure of 38 bar. It was also decided to work with a variable high pressure in order to operate in optimum conditions.

The results obtained for optimal high-pressure values are valid for both systems: refence and subcooling system.

3. Results

3.1. Experimental validation

The setup was validated with energy balance calculation (Table 4) for each of the following components (the gas cooler, the evaporator, the internal heat exchanger in the subcooling system) as well as for the entire system.

The mean expanded uncertainty, calculated using the combined uncertainty method, for water heat transferred is 0.64 kW, while for CO_2 in the gas cooler it is 1.48 kW. It is 0.59 kW for MEG heat transferred, 0.15 kW for the electrical resistance and 1.65 kW for the CO_2 in the evaporator. In the subcooler, the mean expanded uncertainty for the high-pressure CO_2 is 1.01 kW, and it is 0.16 kW for the CO_2 at medium pressure.

The maximum difference between energy balances, for a water inlet temperature between 15 °C and 35 °C, was 0.07 kW in the gas cooler, it was 0.52 kW in the evaporator, it was 0.08 kW in the subcooler and it was 1.41 kW for the global energy balance.

As there is no significant difference, less than 1.77 %, between the three measures of the cooling capacity in the evaporator, it was decided to take the measurements of the electrical resistance power for the calculation of the COP (Eq. (5)) since they are more accurate.

3.2. Thermodynamic analysis

3.2.1. Heat transferred in the subcooler

Fig. 7 shows the temperature difference between the inlet and outlet of the subcooler at the high-pressure side (red dots) and the medium-pressure side (blue dots). Fig. 8 shows the mass flow through the subcooler for the high-pressure side (red dots) and the medium-pressure side (blue dots). Fig. 9 shows the heat transferred in the subcooler at different water inlet temperatures. For the sake of clarity, only four error bars are showed in the figure.

It is observed in Fig. 7 that the temperature difference, between inlet and outlet of the subcooler, increases more rapidly on the medium-pressure side than on the high-pressure side with the gas cooler water inlet temperature. These phenomena could be explained as follows.

The vapor quality (point 5 in Fig. 5) increases with increasing gas cooler water inlet temperature, leading to a higher mass flow rate through the flash gas valve. The heat transferred is then increased (Fig. 9) with the water inlet temperature.

Table 4
Energy balance equations.

Component	Energy balance
Gas cooler	$Q_{water\_GC} = Q_{CO_2\_GC}$
	$m_{water}\ cp_{water}\ \Delta T_{water\_GC} = m_{CO_2} \Delta h_{CO_2\_GC}$
Evaporator	$Q_{MEG\_evap} = Q_{CO_2\_evap} = P_{evap\_electric}$
	$m_{MEG}\ cp_{MEG}\ \Delta T_{MEG\_evap} = m_{CO_2} \Delta h_{CO_2\_evap} = P_{evap\_electric}$
Subcooling	$Q_{CO_2\_SC\_HP} = Q_{CO_2\_SC\_MP}$
	$m_{CO_2} \Delta h_{CO_2\_SC\_HP} = m_{CO_2} \Delta h_{CO_2\_SC\_MP}$
Global energy balance	$Q_{evap} + P_{elec} = Q_{GC}$

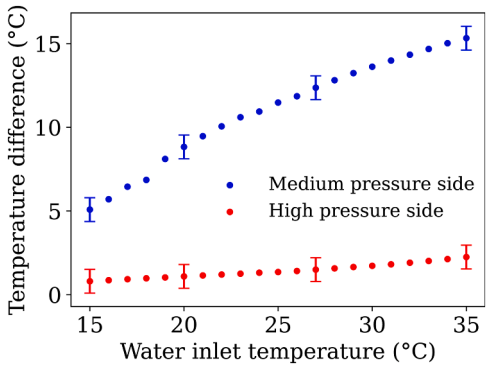

Fig. 7. Temperature difference in the subcooler for the high-pressure side (red dots) and the medium-pressure side (blue dots).

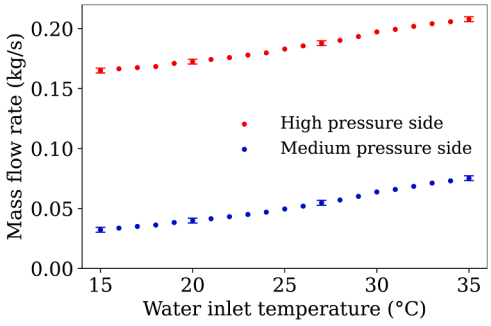

Fig. 8. Mass flow rate through the subcooler for the high-pressure side (red dots) and the medium-pressure side (blue dots).

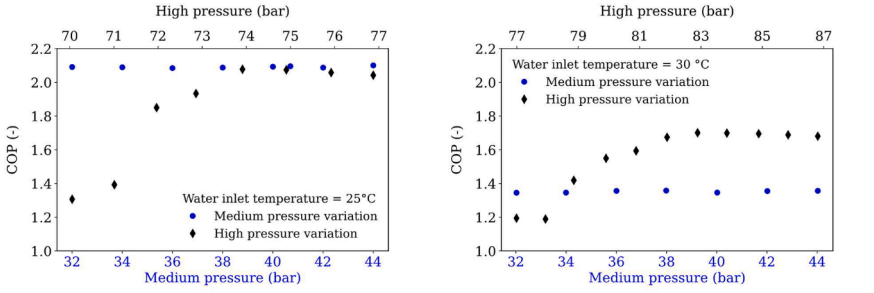

a) Influence of high and medium pressures on COP at 25 °C

b) Influence of high and medium pressures on COP at 30 °C

Fig. 6. Comparison of the influence of high and medium pressures on COP for two different conditions (gascooler water inlet temperature of 25 and 30 °C).

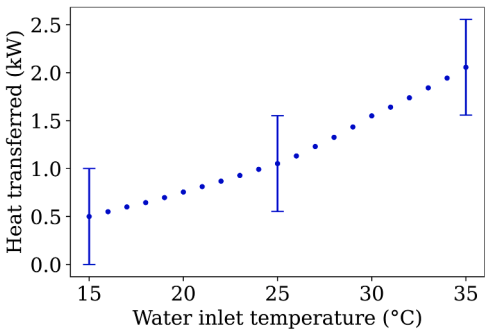

Fig. 9. Heat transferred in the subcooler at different water inlet temperatures.

The heat absorbed by the vapor coming from the receiver (point 6 to 7 in Fig. 5) equals the heat rejected by the fluid coming from the gas cooler (point 3 to 4 in Fig. 5). However, the mass flow rate and the state of the fluid on each side of the subcooler differ (Fig. 8). The total mass flow rate passes through the high-pressure side of the internal heat exchanger, while only a part of the total mass flow rate passes through the medium-pressure side (the total mass flow is the flow passing through the compressors).

The fluid exiting the gas cooler is in a liquid state or in a supercritical state (which has a liquid-like behavior) while the fluid coming out from the receiver is in a saturated vapor state. The specific heat capacity of the vapor is lower than the liquid one. Consequently, the vapor presents rapid temperature increases with only a small amount of added heat, unlike the liquid, which can absorb more heat with minimal temperature change. This explains the two behaviors observed in Fig. 7.

To sum up, the high-pressure side of the subcooler handles a larger total mass flow rate than the medium-pressure side of the subcooler, and it has a higher specific heat capacity. This results in less temperature difference for a given heat transferred.

3.2.2. *Impact of the subcooler on the total and evaporator mass flow rates*

Fig. 10 shows the mass flow rates through the evaporator (crosses) and the total mass flow rates (dots). The three represented systems are:

- the reference system (superheat of 8 °C; black),
- the subcooling system using a reduced superheat (red),
- the subcooling system using a superheat of 8 °C (blue).

For the sake of clarity, only four error bars are showed in the figure, but they are representative of the uncertainties of all the experimental results.

Three phenomena can be observed:

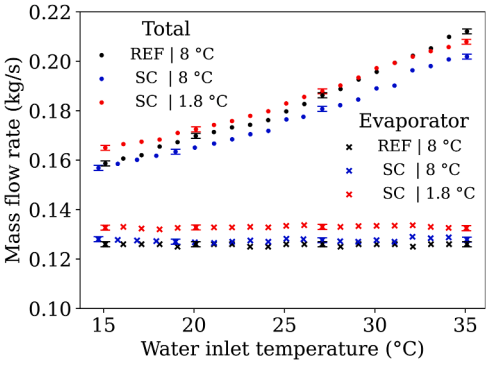

Fig. 10. Evaporator mass flow rate and total mass flow rate for subcooling and reference systems. The evaporator superheat corresponding to each configuration is shown in the figure.

- The mass flow rate through the evaporator (crosses) remains constant whatever the gas cooler water inlet temperature, but the total mass flow rate in the system (dots) increases with the water inlet temperature.
- The total mass flow rates of the subcooling system with a superheat of 8 °C (blue dots), are lower than the reference system ones (black dots). The difference in total mass flow rates between these two systems is greater at high water inlet temperatures than at low water inlet temperatures.
- The total mass flow rates of the subcooling system with a reduced evaporator superheat (red dots) are higher than the reference system ones (black dots), except for water inlet temperatures above 30 °C.

These three phenomena could be explained as follows, respectively:

- The first observation occurs for two reasons. Firstly, the cooling capacity of the system remains constant, as explained in Section 2.4, with the increase of the water inlet temperature, hence the evaporator mass flow rate for a given system. Secondly, as the water inlet temperature increases, the vapor quality at the liquid receiver (point 5 in Fig. 7) increases. Consequently, the mass flow rate through the flash gas valve increases with water inlet temperature. To keep the cooling capacity constant (30 kW), the total mass flow rate must be increased with the inlet water temperature.
- The addition of a subcooler reduces the liquid receiver (LR) inlet vapor quality (point 5, Fig. 5(b)), compared to the reference system. Consequently, this reduction in vapor quality decreases the mass flow rate at the flash gas valve (FGV). This explains that the blue dots are under the black dots.

  The mass flow rate reduction in the flash gas valve also depends on the heat transferred in the subcooler. The heat transferred increases with the water inlet temperature. It means a further reduction in mass flow rate at the flash gas valve at high inlet water temperature.

  Given that the mass flow rate in the evaporator remains constant, any reduction in the mass flow rate at the flash gas valve directly decreases the total mass flow rate. For that reason, the difference in total mass flow rates between subcooling and reference systems is greater at high water inlet temperatures than at low water inlet temperatures.

- The reduction of the flash gas mass flow rate with the subcooler has been explained before. Furthermore, to reduce the evaporator superheat, a higher mass flow rate through the evaporator is required (red crosses). The total mass flow rate is affected by the reduction of the mass flow rate at the flash gas valve and the increase of the mass flow rate at the evaporator.

  At low water inlet temperatures, the reduction of flash gas mass flow rate is low, then the total mass flow rate difference is mainly influenced by the increase of the mass flow rate in the evaporator. This explains that the red dots are above the black dots at low water inlet temperatures.

  At high water inlet temperatures, the reduction of flash gas mass flow rate is high, such that with our experimental setup, it is observed that the total mass flow rate becomes lower than the reference system.

3.2.3. *Coefficient of performance*

Fig. 11 shows the coefficient of performance for the reference system with a superheat of 8 °C (blue dots), the subcooling system with a superheat of 8 °C (blue dots) and the subcooling system with a reduced superheat of 1.8 °C (red dots). Some uncertainties bars are depicted.

A COP enhancement is observed using a subcooler system at the same evaporator superheat of 8 °C (blue dots are above black dots), it is explained by the reduction of the total mass flow rate in the system for the same needs, same cooling capacity and same MEG temperatures. This mass flow rate reduction results in a compressor power reduction.

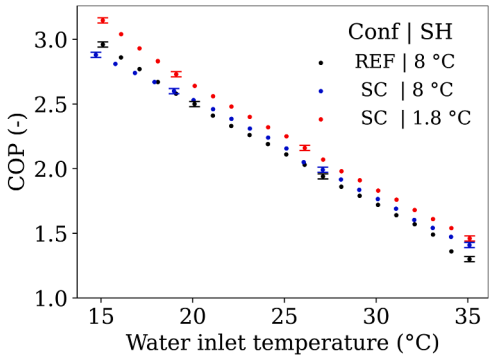

Fig. 11. COP for the reference system and the subcooling system at superheat of 1.8 and 8 °C. Cooling capacity: 30 kW.

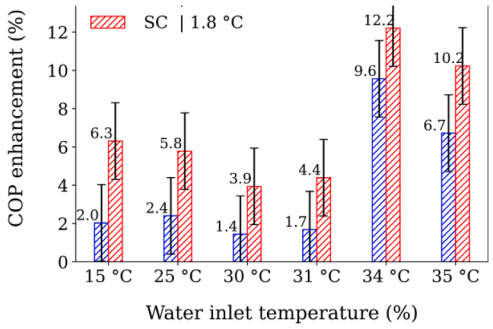

Fig. 12. COP enhancement between the subcooling system and the reference system.

Furthermore, using a subcooling system with a reduced superheat is more interesting than one with a high superheat, because it also increases the evaporator low-pressure. Reducing the superheat without risking compressor damage is possible thanks to the benefits offered by a subcooler.

Fig. 12 shows the COP enhancement for four different gas cooler water inlet temperatures for the subcooling system compared with the reference system using a superheat of 1.8 and 8 °C. It is observed that the COP enhancement is more significant at higher water inlet temperatures than at lower temperatures. This finding aligns with existing literature, but not in all cases. (Aprea and Maiorino, 2008) show the contrary: the greater COP enhancement using an internal heat exchanger is achievable at lower secondary fluid temperatures in the gas cooler. It is because the internal heat exchanger has a different thermal influence depending on its geometry and its position in the cycle.

Different arrangements have been described in the literature which use internal heat exchangers to improve the efficiency of the system. However, all these systems result in a considerable superheat at the compressor inlet, which degrades the efficiency of the compressor.

The solution proposed in this article has the advantage that the low-pressure fluid coming from the subcooler is cooled by the fluid leaving the evaporator before entering the compressor.

(Sánchez et al., 2014) evaluated the classic position of the internal heat exchanger (IHX) for a single stage system, IHX between the gas cooler and the evaporator outlet, and they found a COP enhancement of 1.1% for 25 °C, and 10.7% for 35 °C. (Torrella et al., 2011) reported an enhancement around 6% at 31 °C and around 8% at 34 °C, for the same IHX position. (Aprea and Maiorino, 2008) reported a COP enhancement of 10.3% at 30 °C and 7.1% at 35 °C, for the same classic position. (Karampour and Sawalha, 2014) tested nine different positions of the internal heat exchanger and they do not find a significant improvement of the COP, less than 2%. Finally, (S. X. Liu et al., 2021) tested three different configurations using an internal heat exchanger and they found COP changes between −3.75% and +6.48% for ambient temperatures between -5 °C to 40 °C. At 30 °C the highest COP enhancement that they found was around 2% and at 35 °C was around 3%. The proposed system does not always present higher COP improvements compared to other systems, but in many cases it does. This finding encourages further research of this new position for the internal heat exchanger in CO_2 refrigeration systems.

4. Conclusions

A new arrangement of CO_2 refrigeration systems is proposed to improve the performances for supermarket applications. It consists in using an internal heat exchanger placed at the outlet of the gas cooler and using the saturated vapor leaving the liquid receiver, along with a reduced superheat. An experimental study has been carried out comparing the performances between a subcooling system and a reference system in steady state conditions.

The experimental study has been performed in a 30 kW cooling capacity CO_2 refrigeration prototype. The water inlet temperature in the gas cooler (hot sink) varied between 15 °C and 35 °C. The monoethylene glycol outlet temperature (cold source) from the evaporator was fixed at -8 °C.

The subcooling system, in combination with a reduced evaporator superheat, showed a coefficient of performance (COP) improvement of 10.2 % under transcritical conditions and 6.3 % under subcritical conditions compared to the reference system. However, when using a subcooling system with a high evaporator superheat, the enhancement was reduced to 6.7% and 2 % for the same conditions, respectively.

Declaration of competing interest

The authors declare that they have no known competing financial interests or personal relationships that could have appeared to influence the work reported in this paper.

Acknowledgment

This work was supported by the electricity of France (EDF) (projet number P125P).

Supplementary materials

Supplementary material associated with this article can be found, in the online version, at doi:10.1016/j.ijrefrig.2024.03.010.

Appendix. Experimental results

The uncertainty of the data considers the Type A and Type B uncertainties. The results in Table 5 have a confidence level of 95%, a coverage factor of 2 is considered.

Where T_in_GC is the water inlet gas cooler temperature, HP is the high pressure, MP is the receiver pressure, LP is the low pressure, MEG_in_HX is the MEG inlet evaporator temperature, MEG_out_HX is the MEG outlet evaporator temperature, MEG_m is the MEG mass flow rate, CO_2_out_HX is the CO_2 outlet evaporator temperature, CO_2_in_CP is the CO_2 compressor inlet temperature, CO_2_out_CP is the CO_2 compressor outlet temperature, CO_2_out_GC is the CO_2 gas cooler outlet temperature, P_{elec} is the electric power and P_{evap} is the cooling capacity.

Table 5
Experimental results of the subcooling and reference systems.

Conf $u(x_i)$	T_in_GC (°C) (± 0.073)	HP (bar) (± 0.85)	LP (bar) (± 0.25)	MEG_in_HX (°C) (± 0.070)	MEG_out_HX (°C) (± 0.070)	MEG_m (kg/s) (± 0.015)	CO_2_out_HX (°C) (± 0.37)	Superheat (°C) (± 0.37)	CO_2_in_CP (°C) (± 0.37)	CO_2_out_CP (°C) (± 0.71)	CO_2_out_GC (°C) (± 0.71)	P_{elec} (kW) (± 0.10)	Q_{evap} (kW) (± 0.10)	COP (-) (± 0.016)
SC	15.1	60.81	25.9	−4.85	−8.6	2.24	−8.98	1.79	−9.65	62.47	20.06	9.4	29.54	3.15
SC	16.1	62.16	25.92	−4.78	−8.53	2.24	−8.91	1.84	−9.46	64.42	20.7	9.75	29.6	3.04
SC	17.1	63.46	25.94	−4.79	−8.54	2.24	−8.92	1.81	−9.32	66.59	21.33	10.09	29.52	2.93
SC	18.1	64.61	25.96	−4.78	−8.52	2.23	−8.92	1.79	−9.19	68.8	21.89	10.39	29.4	2.83
SC	19.1	65.91	25.94	−4.79	−8.54	2.24	−8.95	1.78	−9.16	70.49	22.51	10.8	29.55	2.74
SC	20.11	67.28	25.97	−4.76	−8.5	2.24	−8.91	1.78	−8.95	72.58	23.16	11.17	29.53	2.64
SC	21.1	68.67	26.01	−4.73	−8.47	2.24	−8.88	1.76	−8.75	74.79	23.81	11.57	29.56	2.56
SC	22.1	70.04	26.04	−4.72	−8.46	2.24	−8.86	1.74	−8.62	76.82	24.48	11.95	29.52	2.47
SC	23.11	71.48	26.07	−4.65	−8.4	2.24	−8.8	1.77	−8.36	78.89	25.16	12.37	29.58	2.39
SC	24.11	72.96	26.1	−4.62	−8.37	2.25	−8.77	1.75	−8.13	81	25.86	12.8	29.58	2.31
SC	25.1	74.38	26.09	−4.59	−8.33	2.26	−8.78	1.75	−7.91	83.7	26.52	13.3	29.62	2.23
SC	26.09	76.19	26.09	−4.6	−8.36	2.26	−8.76	1.77	−7.47	86.73	27.38	13.94	29.7	2.13
SC	27.1	78.12	26.14	−4.53	−8.27	2.26	−8.69	1.77	−7.22	89.05	28.32	14.46	29.59	2.05
SC	28.09	80.19	26.17	−4.52	−8.26	2.25	−8.64	1.78	−7.06	91.63	29.29	15.08	29.55	1.96
SC	29.09	82.21	26.21	−4.43	−8.17	2.26	−8.55	1.82	−6.7	94.32	30.25	15.73	29.6	1.88
SC	30.09	84.08	26.27	−4.35	−8.09	2.26	−8.5	1.78	−6.37	96.9	31.2	16.38	29.63	1.81
SC	31.09	86.43	26.32	−4.32	−8.06	2.26	−8.43	1.79	−6.14	99.87	32.15	17.1	29.64	1.74
SC	32.09	88.8	26.39	−4.28	−8.01	2.26	−8.39	1.74	−5.88	102.92	33.08	17.84	29.62	1.66
SC	33.09	91.11	26.46	−4.19	−7.89	2.26	−8.3	1.74	−5.69	105.55	34.02	18.49	29.49	1.6
SC	34.08	93.51	26.49	−4.21	−7.91	2.26	−8.29	1.71	−5.56	108.62	34.98	19.32	29.45	1.53
SC	35.06	95.94	26.5	−4.19	−7.9	2.25	−8.25	1.73	−5.42	111.91	35.95	20.26	29.44	1.46
SC	15.1	60.56	25.06	−4.64	−8.39	2.24	−4.03	7.9	0.23	78.02	19.93	9.8	29.6	3.02
SC	16.09	61.86	25.08	−4.63	−8.39	2.24	−4.01	7.89	0.3	80.12	20.56	10.15	29.62	2.92
SC	17.1	63.24	25.1	−4.61	−8.36	2.24	−3.98	7.89	0.4	82.14	21.2	10.48	29.57	2.82
SC	18.09	64.59	25.13	−4.58	−8.33	2.24	−3.93	7.9	0.52	84.16	21.85	10.85	29.6	2.73
SC	18.98	65.64	24.98	−4.66	−8.46	2.26	−4.25	7.8	−0.92	89.46	22.36	11.54	30.01	2.6
SC	20.12	67.05	24.87	−4.68	−8.5	2.28	−4.38	7.81	−2.28	86.14	23.02	11.97	30.32	2.54
SC	21.11	68.53	25.01	−4.61	−8.4	2.26	−4.17	7.82	−1.2	88.66	23.73	12.21	30.06	2.46
SC	22.11	69.96	25.06	−4.57	−8.36	2.27	−4.12	7.82	−1.08	90.65	24.4	12.62	30.07	2.38
SC	23.12	71.34	25.1	−4.54	−8.34	2.27	−4.09	7.78	−0.96	92.63	25.1	13.05	30.12	2.31
SC	24.11	72.86	25.13	−4.5	−8.29	2.27	−4.04	7.8	−0.81	94.65	25.78	13.43	30.05	2.24
SC	25.11	74.16	25.06	−4.41	−8.19	2.28	−4.14	7.79	−1.66	96.29	26.39	14	30.14	2.16
SC	26.1	76.04	25.12	−4.33	−8.1	2.28	−4.01	7.84	−0.97	99.15	27.29	14.51	30	2.07
SC	27.09	77.79	25.09	−4.33	−8.07	2.29	−4.05	7.84	−1.74	100.63	28.14	15.01	29.9	1.99
SC	28.08	79.82	25.18	−4.32	−8.06	2.29	−3.93	7.84	−1.3	103.63	29.09	15.55	29.79	1.92
SC	29.08	81.86	25.25	−4.26	−7.98	2.29	−3.87	7.8	−0.93	106.58	30.05	16.17	29.71	1.84
SC	30.09	83.72	25.31	−4.09	−7.82	2.3	−3.78	7.8	−0.84	108.78	31.04	16.92	29.83	1.76
SC	31.08	86.07	25.39	−4.09	−7.8	2.29	−3.68	7.8	−0.4	112.31	31.98	17.58	29.72	1.69
SC	32.08	88.64	25.46	−3.96	−7.63	2.28	−3.51	7.86	0.76	116.36	32.99	18.1	29.45	1.63
SC	33.1	91.29	25.59	−3.97	−7.67	2.26	−3.42	7.78	−0.86	120.96	34.08	18.91	29.44	1.56
SC	34.1	93.64	25.6	−3.86	−7.55	2.26	−3.33	7.86	−0.71	124.16	35.03	19.77	29.45	1.49
SC	35.09	95.69	25.08	−4.13	−7.87	2.29	−4.1	7.86	−0.12	126.45	21.57	35.83	29.9	1.41
REF	15.1	60.75	24.79	−5.01	−8.78	2.23	−4.52	7.78	−6.64	71.26	20.02	9.97	29.53	2.96
REF	16.09	62.1	24.82	−4.97	−8.74	2.23	−4.46	7.81	−6.72	72.91	20.65	10.33	29.57	2.86
REF	17.1	63.4	24.84	−4.96	−8.73	2.23	−4.46	7.77	−6.81	74.76	21.29	10.68	29.51	2.77
REF	18.1	64.79	24.88	−4.96	−8.72	2.23	−4.42	7.76	−7.54	75.98	21.96	11.08	29.52	2.67
REF	19.09	66.15	24.9	−4.92	−8.68	2.23	−4.38	7.77	−7.73	77.46	22.61	11.44	29.49	2.58
REF	20.11	67.09	24.78	−5.09	−8.85	2.26	−4.53	7.79	−7.38	79.84	23.04	11.83	29.72	2.51
REF	21.1	68.93	24.96	−4.88	−8.64	2.23	−4.33	7.74	−7.94	81.02	23.94	12.24	29.49	2.41
REF	22.1	69.98	24.89	−4.98	−8.73	2.26	−4.42	7.75	−7.67	83.14	24.44	12.62	29.63	2.35
REF	23.1	71.73	25	−4.78	−8.51	2.23	−4.23	7.78	−7.96	84.47	25.29	13.02	29.4	2.26
REF	24.1	72.9	24.96	−4.89	−8.64	2.26	−4.31	7.76	−7.78	86.48	25.81	13.43	29.58	2.2
REF	25.04	73.98	24.96	−4.56	−8.23	2.29	−4.28	7.78	−6.61	90	26.29	13.92	29.27	2.11
REF	26.07	75.92	25.01	−4.5	−8.22	2.29	−4.16	7.84	−5.77	90.69	27.22	14.49	29.62	2.04

(*continued on next page*)

Table 5 (*continued*)

Conf $u(x_i)$	T_in_GC (°C) (± 0.073)	HP (bar) (± 0.85)	LP (bar) (± 0.25)	MEG_in_HX (°C) (± 0.070)	MEG_out_HX (°C) (± 0.070)	MEG_m (kg/s) (± 0.015)	CO_2_out_HX (°C) (± 0.37)	Superheat (°C) (± 0.37)	CO_2_in_CP (°C) (± 0.37)	CO_2_out_CP (°C) (± 0.71)	CO_2_out_GC (°C) (± 0.71)	P_{elec} (kW) (± 0.10)	Q_{evap} (kW) (± 0.10)	COP (-) (± 0.016)
REF	27.07	77.9	25.05	−4.42	−8.14	2.29	−4.07	7.87	−5.32	93.1	28.18	15.1	29.64	1.96
REF	28.07	79.9	25.13	−4.36	−8.07	2.29	−4.01	7.82	−5.86	95.26	29.13	15.68	29.59	1.89
REF	29.06	81.98	25.23	−4.22	−7.93	2.29	−3.89	7.81	−5.58	97.64	30.1	16.36	29.62	1.81
REF	30.08	83.86	25.29	−4.23	−7.94	2.3	−3.8	7.81	−6.12	99.75	31.1	17.05	29.63	1.74
REF	31.07	86.24	25.35	−4.05	−7.74	2.29	−3.7	7.83	−5.06	102.51	32.05	17.8	29.55	1.66
REF	32.1	89.31	25.3	−4.42	−8.14	2.24	−3.84	7.76	−8.77	104.69	33.28	18.73	29.42	1.57
REF	33.1	91.63	25.3	−4.4	−8.12	2.24	−3.82	7.77	−8.82	107.8	34.23	19.68	29.38	1.49
REF	34.1	94.05	25	−4.81	−8.56	2.23	−4.29	7.72	−9.34	112.69	35.19	21.65	29.43	1.36
REF	35.09	96.48	24.91	−4.91	−8.64	2.23	−4.36	7.78	−9.53	116.86	36.14	22.6	29.34	1.32

References

Aprea, C., Maiorino, A., 2008. An experimental evaluation of the transcritical CO2 refrigerator performances using an internal heat exchanger. Int. J. Refrig. 31, 1006–1011. https://doi.org/10.1016/j.ijrefrig.2007.12.016.

Ballot-Miguet, B., Blancarte, J., Duhot, G., 2016. Easy Advanced Control for energy efficiency applied to refrigeration. In: ECOS 2016 - The 29th International Conference on Efficiency, Cost, Optimization. Simulation and Environmental Impact of Energy Systems. Slovenia.

Cabello, R., Sánchez, D., Llopis, R., Torrella, E., 2008. Experimental evaluation of the energy efficiency of a CO2 refrigerating plant working in transcritical conditions. Appl. Therm. Eng. 28, 1596–1604. https://doi.org/10.1016/j.applthermaleng.2007.10.026.

Cavalleri, Paolo, De Bona, Mario, Mazzola, D., 2019. Refrigeration Plant With Multiple Evaporatoin Levels and Method of Managing Such a Plant. US201716301231 20170516.

Cavalleri, Paolo, De Bona, Mario, Mazzola, D., 2016. Refrigeration Plant With Multiple Evaporatoin Levels and Method of Managing Such a Plant. AU20160101310 20160728.

Changenet, C., Charvet, J.N., Géhin, D., Sicard, F., Charmel, B., 2008. Study on predictive functional control of an expansion valve for controlling the evaporator superheat. Proc. Inst. Mech. Eng. Part I J. Syst. Control Eng. 222, 571–582. https://doi.org/10.1243/09596518JSCE566.

Chesi, A., Esposito, F., Ferrara, G., Ferrari, L., 2014. Experimental analysis of R744 parallel compression cycle. Appl. Energy 135, 274–285. https://doi.org/10.1016/j.apenergy.2014.08.087.

Dai, B., Zhao, R., Liu, S., Xu, T., Qian, J., Wang, X., Yang, P., Wang, D., 2023. CO2 system integrated with ejector and mechanical subcooling: a comprehensive assessment. Appl. Therm. Eng. 234, 121269 https://doi.org/10.1016/j.applthermaleng.2023.121269.

Deng qiang, J., Jiang xue, P., Lu, T., Lu, W., 2007. Particular characteristics of transcritical CO2 refrigeration cycle with an ejector. Appl. Therm. Eng. 27, 381–388. https://doi.org/10.1016/j.applthermaleng.2006.07.016.

Elbarghthi, A.F.A., Hafner, A., Banasiak, K., Dvorak, V., 2021. An experimental study of an ejector-boosted transcritical R744 refrigeration system including an exergy analysis. Energy Convers. Manag. 238 https://doi.org/10.1016/j.enconman.2021.114102.

Elbel, S., Hrnjak, P., 2004. Effect of Internal Heat Exchanger on performance of transcritical CO2 systems with ejector. Int. Refrig. Air Cond. Conf. R166, 1–8.

Fallahsohi, H., Changenet, C., Place, S., Duhot, G., Ligeret, C., lin shi, X., 2010a. Energy Savings With Advanced Control of Reciprocating Liquid Chillers.

Fallahsohi, H., Changenet, C., Placé, S., Ligeret, C., Lin-Shi, X., 2010b. Predictive functional control of an expansion valve for minimizing the superheat of an evaporator. Int. J. Refrig. 33, 409–418. https://doi.org/10.1016/j.ijrefrig.2009.10.008.

Fangtian, S., Yitai, M., 2011. Thermodynamic analysis of transcritical CO2 refrigeration cycle with an ejector. Appl. Therm. Eng. 31, 1184–1189. https://doi.org/10.1016/j.applthermaleng.2010.12.018.

Gullo, P., Cortella, G., Minetto, S., Polzot, A., 2016. Overfed evaporators and parallel compression in commercial R744 booster refrigeration systems - An assessment of energy benefits. Refrig. Sci. Technol. 261–268. https://doi.org/10.18462/iir.gl.2016.1039.

Gullo, P., Hafner, A., Cortella, G., 2017. Multi-ejector R744 booster refrigerating plant and air conditioning system integration – A theoretical evaluation of energy benefits for supermarket applications. Int. J. Refrig. 75, 164–176. https://doi.org/10.1016/j.ijrefrig.2016.12.009.

Hafner, A., Försterling, S., Banasiak, K., 2014. Multi-ejector concept for R-744 supermarket refrigeration. Int. J. Refrig. 43, 1–13. https://doi.org/10.1016/j.ijrefrig.2013.10.015.

Haida, M., Smolka, J., Hafner, A., Palacz, M., Ostrowski, Z., Bodys, J., Kriezi, E.K., Försterling, S., Nowak, A.J., Banasiak, K., 2020. Performance operation of liquid ejectors for a R744 integrated multi-ejector supermarket system using a hybrid ROM. Int. J. Refrig. 110, 58–74. https://doi.org/10.1016/j.ijrefrig.2019.10.020.

IPCC, 2023. Climate Change 2023: synthesis Report. In: Lee, H., Romero, J. (Eds.), Contribution of Working Groups I, II and III to the Sixth Assessment Report of the Intergovernmental Panel On Climate Change [Core Writing Team. IPCC, Geneva, Switzerland. https://doi.org/10.59327/IPCC/AR6-9789291691647.001 (eds.)] Geneva, Switzerland.

Karampour, M., Sawalha, S., 2014. Investigation of using internal heat exchangers in CO2 trans-critical booster system. In: 11th IIR Gustav Lorentzen Conf. Nat. Refrig. Nat. Refrig. Environ. Prot. GL 2014, pp. 453–460.

Kim, Mo Se, Kang, D.H., Kim, Min Soo, Kim, M., 2017. Investigation on the optimal control of gas cooler pressure for a CO2 refrigeration system with an internal heat exchanger. Int. J. Refrig. 77, 48–59. https://doi.org/10.1016/j.ijrefrig.2017.03.002.

Kim, S.G., Kim, Y.J.Y., Lee, G., Kim, M.S., Cho, H., Ryu, C., Kim, Y.J.Y., 2005. Cooling performance of a variable speed CO2 cycle with an electronic expansion valve and internal heat exchanger. Int. J. Refrig. 28, 664–671. https://doi.org/10.1016/j.ijrefrig.2006.10.004.

Ksayer, E.B., Clodic, D., 2006. Enhancement of CO2 Refrigeration Cycle Using an Ejector : 1D Analysis. Int. J. Refrig. Air Cond. Conf. - Purdue Univ. R058, 1–8.

Li, D., Groll, E.A., 2005. Transcritical CO2 refrigeration cycle with ejector-expansion device. Int. J. Refrig. 28, 766–773. https://doi.org/10.1016/j.ijrefrig.2004.10.008.

Liu, F., Groll, E.A., Li, D., 2012. Modeling study of an ejector expansion residential CO 2 air conditioning system. Energy Build. 53, 127–136. https://doi.org/10.1016/j.enbuild.2012.07.008.

Liu, S., Wang, J., Dai, B., Yang, X., Nian, V., Li, H., Yuan, J., 2021a. Alternative positions of internal heat exchanger for CO2 booster refrigeration system: thermodynamic analysis and annual thermal performance evaluation. Int. J. Refrig. 131, 1016–1028. https://doi.org/10.1016/j.ijrefrig.2021.05.003.

Liu, X., Yu, K., Wan, X., Li, X., 2021b. Performance evaluation of CO2 supermarket refrigeration system with multi-ejector and dedicated mechanical subcooling. Energy Reports 7, 5214–5227. https://doi.org/10.1016/j.egyr.2021.08.110.

Llopis, R., Nebot-Andrés, L., Cabello, R., Sánchez, D., Catalán-Gil, J., 2016. Évaluation expérimentale d'une installation frigorifique transcritique au CO2 avec un sous-refroidissement mécanique dédié. Int. J. Refrig. 69, 361–368. https://doi.org/10.1016/j.ijrefrig.2016.06.009.

Llopis, R., Nebot-Andrés, L., Sánchez, D., Catalán-Gil, J., Cabello, R., 2018. Subcooling methods for CO2 refrigeration cycles: a review. Int. J. Refrig. 93, 85–107. https://doi.org/10.1016/j.ijrefrig.2018.06.010.

Ma, Y., Liu, Z., Tian, H., 2013. A review of transcritical carbon dioxide heat pump and refrigeration cycles. Energy 55, 156–172. https://doi.org/10.1016/j.energy.2013.03.030.

Minetto, S., Brignoli, R., Zilio, C., Marinetti, S., 2014. Experimental analysis of a new method for overfeeding multiple evaporators in refrigeration systems. Int. J. Refrig. 38, 1–9. https://doi.org/10.1016/j.ijrefrig.2013.09.044.

Moffat, R.J., 1982. Contributions to the theory of single-sample uncertainty analysis. J. Fluids Eng. Trans. ASME 104, 250–258. https://doi.org/10.1115/1.3241818.

Nakagawa, Masafumi, Marasigan, A.R., Matsukawa, T., 2011a. Experimental analysis on the effect of internal heat exchanger in transcritical CO2 refrigeration cycle with two-phase ejector. Int. J. Refrig. 34, 1577–1586. https://doi.org/10.1016/j.ijrefrig.2010.03.007.

Nakagawa, M., Marasigan, A.R., Matsukawa, T., 2010. Experimental Analysis of Two-Phase Ejector System With Varying Mixing Cross-Sectional Area Using Natural Refrigerant Co 2. Int. J. Air-Conditioning Refrig. 18, 297–307. https://doi.org/10.1142/s2010132510000320.

Nakagawa, M., Marasigan, A.R., Matsukawa, T., Kurashina, A., 2011b. Experimental investigation on the effect of mixing length on the performance of two-phase ejector for CO2 refrigeration cycle with and without heat exchanger. Int. J. Refrig. 34, 1604–1613. https://doi.org/10.1016/j.ijrefrig.2010.07.021.

Nebot-Andrés, L., 2022. Subcooling systems in transcritical CO2 refrigeration cycles . Experimental evaluation of energy improvement.

Nebot-andrés, L., Calleja-anta, D., Sánchez, D., Cabello, R., Llopis, R., 2022a. Experimental analysis of refrigeration CO2 systems using an additional compressor to enhance energy performance. In: 15th IIR-Gustav Lorentzen Conference on Natural Refrigerants (GL2022). https://doi.org/10.18462/iir.gl2022.0079.

Pardiñas, Á., Selvnes, H., Banasiak, K., Hafner, A., 2023. Next generation of ejector-supported R744 booster systems for commercial refrigeration at all climates. Int. J. Refrig. 148, 168–178. https://doi.org/10.1016/j.ijrefrig.2022.10.027.

Nebot-Andrés, L., Calleja-Anta, D., Sánchez, D., Cabello, R., Llopis, R., 2022b. Experimental assessment of dedicated and integrated mechanical subcooling systems vs parallel compression in transcritical CO2 refrigeration plants. Energy Convers. Manag. 252 https://doi.org/10.1016/j.enconman.2021.115051.

Pardiñas, Á.Á., Fabris, F., Contiero, L., Selvnes, H., Banasiak, K., Hafner, A., 2022. Ejector for the World: simplified ejector-supported CO 2 refrigeration systems for all climates. 15th IIR-Gustav Lorentzen Conf. Nat. Refrig. https://doi.org/10.18462/iir.gl2022.0062.

Rigola, J., Ablanque, N., Pérez-Segarra, C.D., Oliva, A., 2010. Numerical simulation and experimental validation of internal heat exchanger influence on CO2 trans-critical cycle performance. Int. J. Refrig. 33, 664–674. https://doi.org/10.1016/j.ijrefrig.2009.12.030.

Sacasas, D., Vega, J., Cuevas, C., 2022. An annual energetic evaluation of booster and parallel refrigeration systems with R744 in food retail supermarkets . A Chilean perspective. Int. J. Refrig. 133, 326–336. https://doi.org/10.1016/j.ijrefrig.2021.10.010.

Sánchez, D., Patiño, J., Llopis, R., Cabello, R., Torrella, E., Fuentes, F.V., 2014. New positions for an internal heat exchanger in a CO2 supercritical refrigeration plant. Experimental analysis and energetic evaluation. Appl. Therm. Eng. 63, 129–139. https://doi.org/10.1016/j.applthermaleng.2013.10.061.

Sawalha, S., Karampour, M., Rogstam, J., 2015. Field measurements of supermarket refrigeration systems. Part I: analysis of CO2 trans-critical refrigeration systems. Appl. Therm. Eng. 87, 633–647. https://doi.org/10.1016/j.applthermaleng.2015.05.052.

Singh, S., Hafner, A., Maiya, M.P., Banasiak, K., Neksa, P., 2021. Multiejector CO2 cooling system with evaporative gascooler for a supermarket application in tropical regions. Appl. Therm. Eng. 190 https://doi.org/10.1016/j.applthermaleng.2021.116766.

Singh, S., Maiya, P.M., Hafner, A., Banasiak, K., Neksa, P., 2020. Energy efficient multiejector CO2 cooling system for high ambient temperature. Therm. Sci. Eng. Prog. 19, 100590 https://doi.org/10.1016/j.tsep.2020.100590.

Tao, Y.B., He, Y.L., Tao, W.Q., Wu, Z.G., 2010. Experimental study on the performance of CO2 residential air-conditioning system with an internal heat exchanger. Energy Convers. Manag. 51, 64–70. https://doi.org/10.1016/j.enconman.2009.08.024.

Taylor, Barry N, Kuyatt, C.E., 1994. Technology.

Torrella, E., Sánchez, D., Llopis, R., Cabello, R., 2011. Energetic evaluation of an internal heat exchanger in a CO2 transcritical refrigeration plant using experimental data. Int. J. Refrig. 34, 40–49. https://doi.org/10.1016/j.ijrefrig.2010.07.006.

Xu, X.X., Chen, G.M., Tang, L.M., Zhu, Z.J., Liu, S., 2011. Experimental evaluation of the effect of an internal heat exchanger on a transcritical CO2 ejector system. J. Zhejiang Univ. Sci. A 12, 146–153. https://doi.org/10.1631/jzus.A1000212.

Yang, J.L., Ma, Y.T., Li, M.X., Guan, H.Q., 2005. Exergy analysis of transcritical carbon dioxide refrigeration cycle with an expander. Energy 30, 1162–1175. https://doi.org/10.1016/j.energy.2004.08.007.

Yu, B., Yang, J., Wang, D., Shi, J., Chen, J., 2019a. An updated review of recent advances on modified technologies in transcritical CO2 refrigeration cycle. Energy 189. https://doi.org/10.1016/j.energy.2019.116147.

Yu, B., Yang, J., Wang, D., Shi, J., Chen, J., 2019b. An updated review of recent advances on modified technologies in transcritical CO2 refrigeration cycle. Energy 189, 116147. https://doi.org/10.1016/j.energy.2019.116147.

Zhang, Z.Y., Ma, Y.T., Wang, H.L., Li, M.X., 2013. Theoretical evaluation on effect of internal heat exchanger in ejector expansion transcritical CO2 refrigeration cycle. Appl. Therm. Eng. 50, 932–938. https://doi.org/10.1016/j.applthermaleng.2012.08.022.